Covalent Organic Frameworks

How to cite:
International Edition: doi.org/10.1002/anie.202218908
German Edition: doi.org/10.1002/ange.202218908

Enhanced Energy Transfer in A π-Conjugated Covalent Organic Framework Facilitates Excited-State Nickel Catalysis

*Yingjie Fan[+], Dong Won Kang[+], Steven Labalme, Jinhong Li, and Wenbin Lin**

Abstract: Covalent organic frameworks (COFs) have received broad interest owing to their permanent porosity, high stability, and tunable functionalities. COFs with long-range π-conjugation and photosensitizing building blocks have been explored for sustainable photocatalysis. Herein, we report the first example of COF-based energy transfer Ni catalysis. A pyrene-based COF with sp^2 carbon-conjugation was synthesized and used to coordinate Ni^{II} centers through bipyridine moieties. Under light irradiation, enhanced energy transfer in the COF facilitated the excitation of Ni centers to catalyze borylation and trifluoromethylation reactions of aryl halides. The COF showed two orders of magnitude higher efficiency in these reactions than its homogeneous control and could be recovered and reused without significant loss of catalytic activity.

Constructed from organic building blocks via robust periodic covalent bonds, covalent organic frameworks (COFs) have emerged as a promising class of functional porous crystalline materials.[1] COFs have been actively studied in many applications including harmful gas removal, light-mediated therapy, ionic conduction, and catalysis, by taking advantage of their permanent porosity, high stability, and tunable functionalities.[2] Although a diverse array of COFs have been reported with boron-, nitrogen-, and carbon-based linkages,[3] COFs with long-range π-conjugation and organic photosensitizing building blocks have only recently drawn interest as sustainable and cost-effective photocatalysts to replace noble metal photosensitizers.[4] In particular, sp^2-carbon conjugated COFs are actively studied as potential photocatalysts due to their excellent chemical stability and photoluminescence properties.[5]

Despite their potential in fine chemical synthesis, most COF-based photocatalysts have only been examined in photo-induced reactions related to solar energy conversion, such as proton and carbon dioxide reduction.[6] For example, nickel was integrated into a COF for selective reduction of CO_2 into CO.[7] More recently, COFs have been examined in photoredox cross-coupling reactions to form C–N, C–O, and C–S bonds.[8] By merging photoredox and transition metal catalysis, metallaphotoredox catalysis has provided powerful synthetic methodologies for bond formations.[9] However, noble metal-based photosensitizers are typically required in metallaphotoredox catalysis. With molecular tunability, conjugated COFs could serve as sustainable and low-cost substitutes to precious metal-based photosensitizers in metallaphotoredox catalysis.

With the ability to mediate radical-based cross-coupling reactions, Ni has been widely explored in metallaphotoredox catalysis and energy transfer catalysis.[10] Through a comprehensive photophysical study of Ni^{II} complexes, Doyle and co-workers recently identified Ni^{II} complexes in their ^{3}d-d excited states as key intermediates in energy transfer Ni catalysis by weakening the Ni^{II}-aryl bonds to form aryl radicals and Ni^{I} species.[11] Li and co-workers recently reported Ni-catalyzed cross-coupling reactions, including redox neutral C–C and C–X bond formations as well as reductive C–C and C–N bond formations with a Ni complex containing a photoactive ligand.[12] Although the detailed mechanisms were not elucidated for the reactions catalyzed by this two-in-one Ni complex, we envision this strategy can be extended to COF catalysis by introducing Ni centers into conjugated photoactive COFs. The interaction between the conjugated COF and Ni centers may enhance energy transfer from the photoexcited COF to Ni centers to facilitate the generation of aryl radicals for coupling reactions.

Herein, we report the first example of COF-based energy transfer Ni catalysis. A pyrene-based COF with sp^2-carbon conjugation was synthesized through Knoevenagel condensation (Figure 1), and used to coordinate Ni^{II} centers through the bipyridine moieties. Under light irradiation, pyrenes in the COF were photoexcited and efficiently transferred energy to Ni catalytic sites. As a result, the COF efficiently catalyzed radical-based borylation and trifluoromethylation reactions of aryl halides, with two orders of magnitude higher catalytic efficiency than its homogeneous control.

The two-dimensional (2D) sp^2-carbon conjugated COF (**CN**) was prepared via a Knoevenagel reaction between 1,3,6,8-tetrakis(4-formylphenyl)pyrene (py-CHO) and 2,2′-([2,2′-bipyridine]-5,5′-diyl)diacetonitrile (bpy-CN) in o-dichlorobenzene and 1-butanol with 6 M aqueous KOH solution at 120 °C for 72 h (Figure 2a).[5a,13] **CN** was metalated with $NiBr_2$·dme (dme is ethylene glycol dimethyl ether)

[*] Y. Fan,[+] Dr. D. W. Kang,[+] S. Labalme, J. Li, Prof. Dr. W. Lin
Department of Chemistry, The University of Chicago
Chicago, IL-60637 (USA)
E-mail: wenbinlin@uchicago.edu

[+] These authors contributed equally to this work.

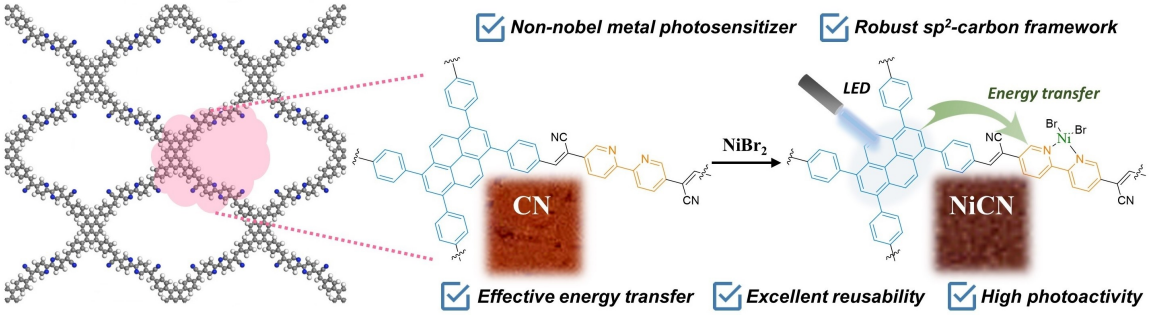

Figure 1. Schematics showing energy transfer catalysis by a sp^2-carbon conjugated COF. Upon photoexcitation, pyrenes in the COF efficiently transfer energy to Ni centers to facilitate radical-based cross coupling reactions by weakening the Ni^{II}-aryl bonds to generate aryl radicals and Ni^{I} species.

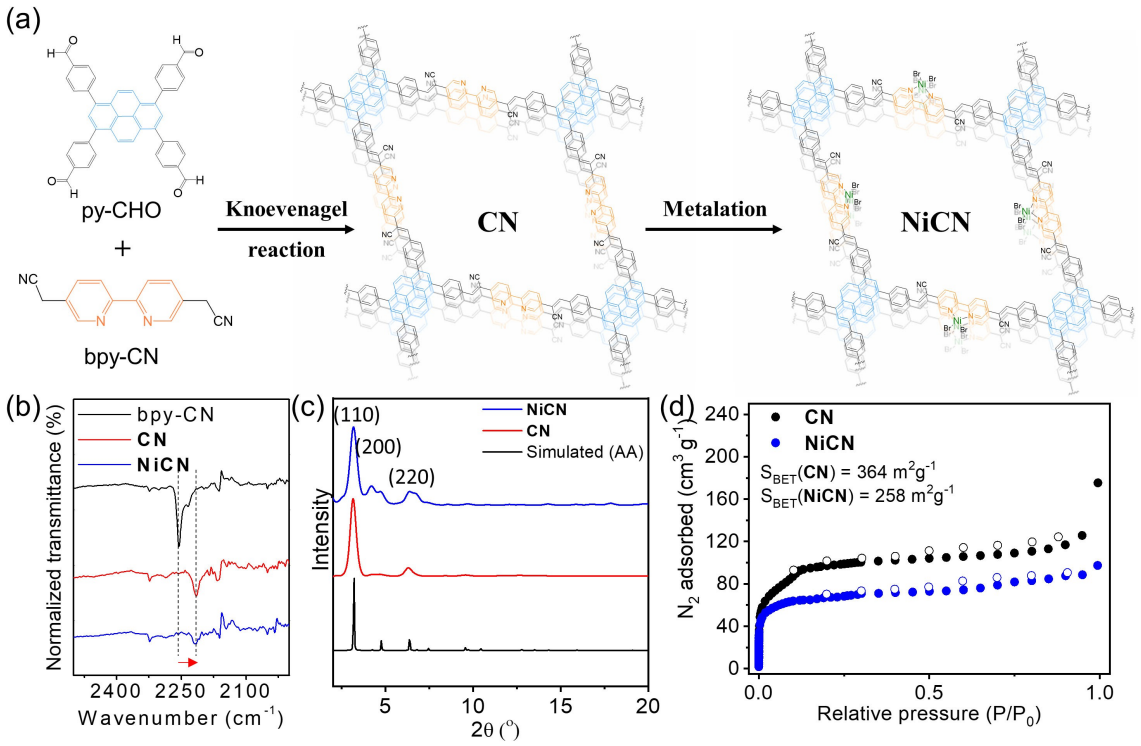

Figure 2. (a) Synthetic scheme for **CN** and **NiCN**. (b) FT-IR spectra of bpy-CN, **CN**, and **NiCN** in the C≡N stretching region. (c) Experimental and simulated PXRD patterns of **CN** and **NiCN** (Background subtraction was performed for better comparison). (d) Nitrogen sorption isotherms for **CN** and **NiCN** at 77 K.

in a 1:1 mixture of *N,N*-dimethylformamide (DMF) and toluene at 60 °C for 24 h to afford **NiCN** for catalytic reactions. After the Knoevenagel reaction, characteristic peaks of aldehyde C–H stretching in py-CHO (2718 cm^{-1}) and C≡N stretching in bpy-CN (2255 cm^{-1}) were not detected. The C=O stretching vibration of py-CHO at 1691 cm^{-1} decreased while the C=C stretching vibration at 1600 cm^{-1} increased (Figure S1). New peaks appeared at 2215 cm^{-1} for **CN** and 2219 cm^{-1} for **NiCN** (Figure 2b), which were assigned to the C≡N stretching in the vinyl cyano group. This assignment was confirmed by solid-state NMR spectroscopy (Figure S2). The spectroscopic data supported the formation of C=C bonds via Knoevenagel condensation and the synthesis of sp^2-carbon conjugated COF.[13]

Powder X-ray diffraction (PXRD) studies were performed to confirm the structure and crystallinity of **CN**. The experimental PXRD pattern of **CN** matched the simulated pattern well and Rietveld refinements showed excellent agreement between the two with $R_p = 2.71\,\%$ and $R_{wp} = 4.39\,\%$. The refinement results further indicated that 2D networks of **CN** eclipsed with each other to afford one-dimensional channels of 2.5 nm in size (Figure 2c, Figure S3 and Table S1). **NiCN** showed a similar PXRD pattern to that of **CN**, which was also in agreement with the simulated result from Pawley refinement ($R_p = 0.62\,\%$ and $R_{wp} =$

1.08 %). X-ray photoelectron spectroscopy (XPS) indicated the presence of Ni and Br in **NiCN** (Figure S5). The Ni $2p_{1/2}$ binding energy of 873.17 eV in **NiCN** suggested the divalent nature of Ni centers. Nitrogen sorption isotherms of the COFs were collected at 77 K after they were degassed at 120 °C under high vacuum for 10 h. Brunauer–Emmett–Teller (BET) surface areas for **CN** and **NiCN** were calculated to be 364 $m^2 g^{-1}$ and 258 $m^2 g^{-1}$, respectively (Figure 2d). The largest pore size of 2.3 nm calculated by the density functional theory method based on the sorption isotherms of **CN** was consistent with the expected 1D channel size formed from eclipsed 2D networks. Transmission electron microscopy (TEM) revealed tubular morphologies of **CN** and **NiCN** with a diameter of approximately 200 nm (Figure S4).

The reactivity of **NiCN** was first studied in energy-transfer mediated cross-coupling reactions between aryl halides and benzoic acid (Figure S13).[10c] Despite many attempts, we observed dehalogenation of a large fraction of aryl halides, which was previously seen in photo-induced reductive elimination from Ni^{II}-aryl complexes.[10c] When DMSO was used as the solvent, a deoxygenated C–S cross-coupled product was obtained, indicating the radical nature of these **NiCN**-catalyzed reactions. These results could be explained by the generation of aryl radicals from Ni^{II}-aryl complexes.

These observations prompted us to examine radical-based borylation reactions and trifluoromethylation reactions of aryl halides with **NiCN**. With diisopropylethylamine (DIPEA) as a base and pyridine as a nucleophile to activate boron agents,[14] 0.5 mol % **NiCN** catalyzed cross-coupling between methyl 4-bromobenzoate (**1b**) and bis(pinacolato)diboron (B_2pin_2) in acetonitrile under 370 nm blue LED light in 16 hours to afford methyl 4-(4,4,5,5-tetramethyl-1,3,2-dioxaborolan-2-yl)benzoate (**2b**) in 78 % yield (Table S2, Figure 3a). Interestingly, 5 mol % of pyrene and 5 mol % of Ni(dtbpy)Br_2 (dtbpy is 4,4′-di-tert-butyl-2,2′-dipyridyl) were needed to obtain **2b** in a comparable yield (63 %, Table S2), indicating that **NiCN** outperformed its homogeneous counterpart by 247 times.

We next explored the substrate scope for **NiCN**-catalyzed borylation reactions of aryl halides. As shown in Table 1a, aryl iodides with electron-withdrawing groups cyano (**1a**), ester (**1b**), pyridine (**1c**), aldehyde (**1d**), and ketone (**1e**) reacted with B_2pin_2 smoothly to yield products **2a–e** in 78–85 % yields. Aryl bromides with the same electron-deficient groups (**1a′–e′**) also worked to give products **2a–e** in slightly lower yields of 61–83 %. Electron-rich aryl iodides, including 1-iodonaphthylene (**1f**), 4-iodotoluene (**1g**), 2-iodothiophene (**1h**), 4-iodoaniline (**1i**), and 4-iodoanisole (**1j**), were also tolerated to give product **2f–j** in 69–92 % yields. The turnover numbers (TONs) ranged from 122 to 184 for borylation reactions.

In the presence of CuI and KF, 0.5 mol % **NiCN** also catalyzed the trifluoromethylation of **1b** with trifluoromethyltrimethylsilane ($TMSCF_3$) in acetonitrile after 370 nm blue LED irradiation for 16 hours to yield methyl 4-trifluoromethyl benzoate (**3b**) in 88 % yield (Table S3). In comparison, 5 mol % of pyrene and 5 mol % of Ni(dtbpy)Br_2 were needed to obtain **3b** in a comparable yield (83 %, Table S3), suggesting that **NiCN** outperformed its homogeneous counterpart by 212 times.

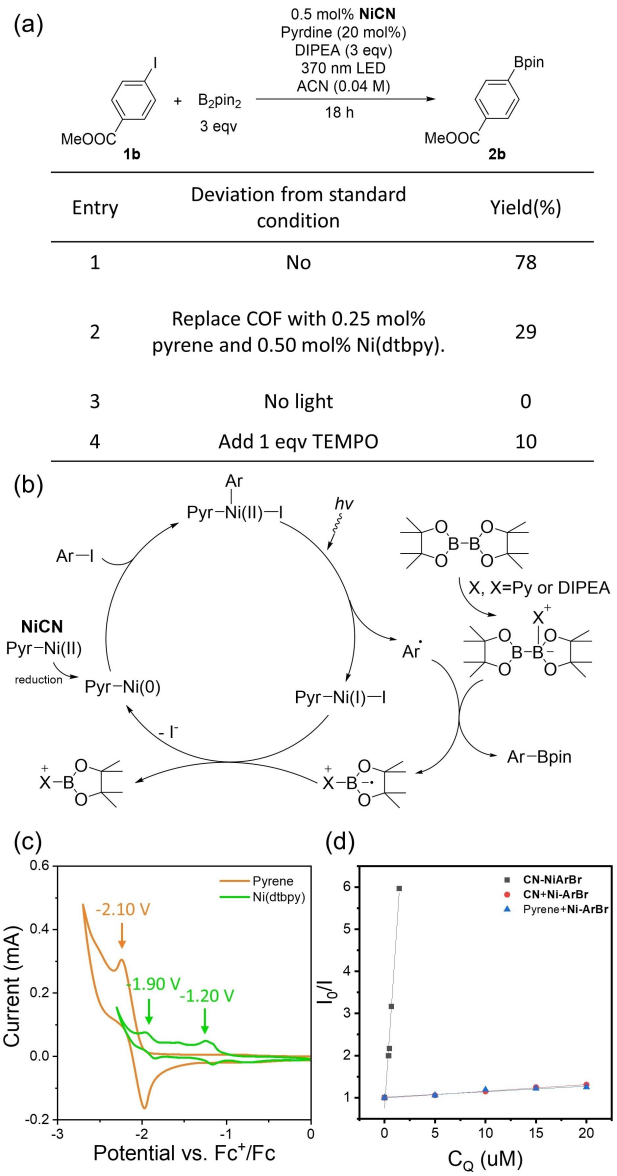

Entry	Deviation from standard condition	Yield(%)
1	No	78
2	Replace COF with 0.25 mol% pyrene and 0.50 mol% Ni(dtbpy).	29
3	No light	0
4	Add 1 eqv TEMPO	10

Figure 3. Mechanistic studies. (a) Control experiments for **NiCN** catalyzed borylation reactions. (b) proposed mechanisms for **NiCN** catalyzed borylation reactions. (c) CV diagram of pyrene and Ni(dtbpy). Redox peaks are shown with arrows and corresponding potentials in the figure. (d) Stern-Völmer plots for quenching of **NiCN(ArBr)**, **CN** and pyrene.

NiCN-catalyzed trifluoromethylation reactions had a broad substrate scope (Table 1b). Aryl iodides (**1a–d**, **1k**) and aryl bromides (**1a′–d′**, **1k′**) with electron-withdrawing cyano, ester, pyridine, carbonyl and nitro groups reacted with $TMSCF_3$ to yield corresponding products **3a–d** and **3k** in 60–88 % yields. Aryl iodides containing electron-donating groups (**1f–i**, **1l**) also reacted with $TMSCF_3$ to afford products **3f–i** and **3l** in 62–82 % yields. The TONs ranged from 124 to 178 for trifluoromethylation reactions. However,

Table 1: **NiCN** catalyzed borylation and trifluoromethylation reactions of aryl halide by energy transfer catalysis.[a]

(a) borylation[b]

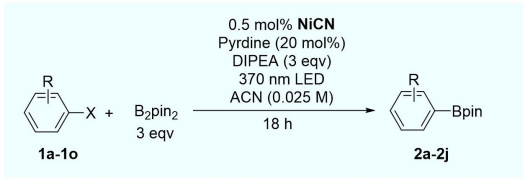

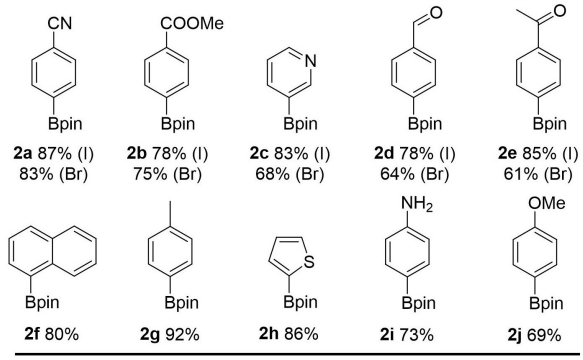

(b) Trifluoromethylation[c]

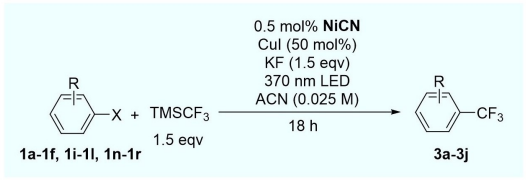

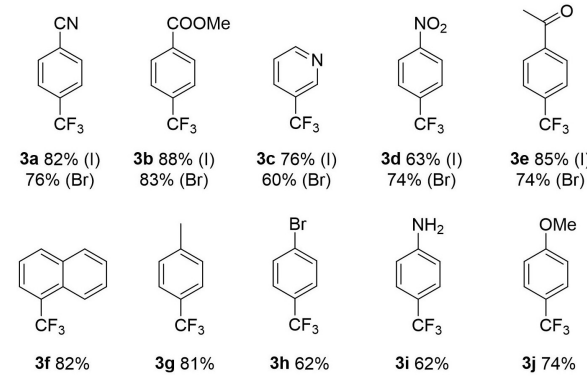

[a] Isolated yields. The parentheses stand for aryl iodide or aryl bromide. [b] Reactions were performed with **1** (0.1 mmol), B_2pin_2 (0.3 mmol), pyridine (0.02 mmol), DIPEA (0.3 mmol) and 50 μmol **NiCN** in 4 mL acetonitrile under 370 nm irradiation for 18 hours. [c] Reactions were performed with **1** (0.1 mmol), $TMSCF_3$ (0.15 mmol), CuI (0.05 mmol), KF (0.15 mmol) and 50 μmol **NiCN** in 4 mL acetonitrile under 370 nm irradiation for 18 hours.

electron-rich aryl bromides did not work for both borylation and trifluoromethylation reactions, likely due to the low oxidative addition ability of electron-poor Ni centers in **NiCN**. **NiCN** was easily recovered from the borylation reaction of **1b** and used in three consecutive cycles without significant loss of catalytic activities and **NiCN** crystallinity (Figure S8), demonstrating the chemical stability and recyclability of the COF catalyst. A total TON of 436 was obtained in the catalyst reuse experiment.

Several control experiments were performed to reveal the mechanisms of **NiCN**-catalyzed borylation and trifluoromethylation reactions (Figure 3a, Table S2, Table S3). First, the addition of TEMPO significantly decreased the product yields for both **NiCN**-catalyzed borylation (from 78 % to 10 %) and trifluoromethylation (from 88 % to 10 %) reactions. Second, no product was observed in the absence of light. Third, as mentioned above, **NiCN** outperformed the homogeneous counterpart by two orders of magnitude in both borylation and trifluoromethylation reactions. These results suggest a strong synergy between pyrenes and Ni centers in **NiCN** and the reactions go through light-mediated radical pathways. Based on literature precedents in weakened Ni^{II}-aryl bonds in their excited states[11] and in photoredox borylation reactions,[15] we propose **NiCN-**catalyzed borylation reactions proceed via energy transfer mechanism (Figure 3b). Ni^{II} is first photoreduced by pyrenes in **NiCN** with DIPEA as a reductant. The resulting Ni^0-bipyridine complex undergoes oxidative addition with aryl halide to form a Ni^{II}-aryl complex. Upon photoexcitation, the pyrene transfers energy to the Ni^{II}-aryl complex to facilitate the cleavage of the Ni–C bond and the generation of an aryl radical, which is captured by B_2pin_2 to afford the borylation product. The rest of B_2pin_2 leaves as a boron radical anion which reduces Ni^I to Ni^0 to complete the catalytic cycle.

Cyclic voltammetry (CV) experiments were performed to support the proposed mechanism (Figure 3c). Reduction potential of pyrene was determined as −2.10 V vs. Fc^+/Fc. $Ni^{II}(dtbpy)Br_2$ showed two reversible reductive peaks at −1.20 V and −1.90 V vs. Fc^+/Fc. With a proper reductive quencher (DIPEA in the borylation reaction), the reduction power of pyrene anion is strong enough to reduce Ni^{II}-bipyridine complex to Ni^0 species. Luminescence studies were performed to analyze energy transfer in **NiCN** (Figure 3d). Free and **CN**-grafted Ni^{II}(aryl)Br complex (**Ni-ArBr** or **NiCN(ArBr)**) were synthesized via oxidation addition of Ni(cod)(bpy) species to 4-bromobenzonitirle.[16] **NiCN-(ArBr)** samples with different Ni loadings were also prepared. Photoluminescence quenching of **NiCN(ArBr)** at different Ni loadings and **CN** or pyrene by different equivalents of **Ni-ArBr** were fitted by Stern-Völmer plots. The energy transfer of **NiCN(ArBr)** was calculated to be 225 times faster than that between **CN** and **Ni-ArBr**, and 7.3×10^5 times faster than that between pyrene and **Ni-ArBr**. Based on the properties of excited Ni^{II}-aryl complexes,[11] enhanced energy transfer in **NiCN** will accelerate the generation of aryl radicals from excited-state Ni^{II}-aryl species and therefore improve the efficiency of radical borylation reactions. A similar mechanism was proposed for radical-based trifluoromethylation reactions (Figure S12), which should also be accelerated by enhanced energy transfer in **NiCN**.

In summary, we have designed a sp^2-carbon conjugated COF for catalytic borylation and trifluoromethylation reactions of aryl halides through energy transfer from the COF to Ni active sites. The crystalline porous COF linked via C=C bonds was synthesized via Knoevenagel condensation, and then coordinated to Ni^{II} centers through the bipyridine

moieties. Photoexcited pyrenes in the COF efficiently transferred energy to Ni catalytic sites to catalyze radical-based borylation and trifluoromethylation reactions of aryl halides. Enhanced energy transfer in this π-conjugated COF greatly facilitates excited-state Ni catalysis with two orders of magnitude higher catalytic efficiency than its homogeneous control. The COF was recycled and reused without significant loss of catalytic activity and crystallinity. This work highlights the potential of COFs in sustainable metallaphotoredox catalysis with Earth-abundant metals.

Acknowledgements

We thank Haifeng Zheng for experimental help. We thank Alexander Filatov for the help with XPS and PXRD measurements. We acknowledge the National Science Foundation (CHE-2102554) and the University of Chicago for funding support and the MRSEC Shared User Facilities at the University of Chicago (DMR-1420709) for instrument Access.

Conflict of Interest

The authors declare no conflict of interest.

Data Availability Statement

The data that support the findings of this study are available from the corresponding author upon reasonable request.

Keywords: Covalent Organic Framework · Energy Transfer · Heterogeneous Photocatalysis · Nickel Catalysis · π-Conjugation

[1] a) J. Jiang, Y. Zhao, O. M. Yaghi, *J. Am. Chem. Soc.* **2016**, *138*, 3255–3265; b) K. Geng, T. He, R. Liu, S. Dalapati, K. T. Tan, Z. Li, S. Tao, Y. Gong, Q. Jiang, D. Jiang, *Chem. Rev.* **2020**, *120*, 8814–8933; c) T. Ma, E. A. Kapustin, S. X. Yin, L. Liang, Z. Zhou, J. Niu, L.-H. Li, Y. Wang, J. Su, J. Li, X. Wang, W. D. Wang, W. Wang, J. Sun, O. M. Yaghi, *Science* **2018**, *361*, 48–52.

[2] a) D. W. Kang, S. E. Ju, D. W. Kim, M. Kang, H. Kim, C. S. Hong, *Adv. Sci.* **2020**, *7*, 2002142; b) J. H. Kim, D. W. Kang, H. Yun, M. Kang, N. Singh, J. S. Kim, C. S. Hong, *Chem. Soc. Rev.* **2022**, *51*, 43–56; c) D. W. Kang, M. Kang, H. Yun, H. Park, C. S. Hong, *Adv. Funct. Mater.* **2021**, *31*, 2100083; d) J. F. Kurisingal, H. Kim, J. H. Choe, C. S. Hong, *Coord. Chem. Rev.* **2022**, *473*, 214835; e) W. Cao, W. D. Wang, H.-S. Xu, I. V. Sergeyev, J. Struppe, X. Wang, F. Mentink-Vigier, Z. Gan, M.-X. Xiao, L.-Y. Wang, G.-P. Chen, S.-Y. Ding, S. Bai, W. Wang, *J. Am. Chem. Soc.* **2018**, *140*, 6969–6977.

[3] a) X. Chen, K. Geng, R. Liu, K. T. Tan, Y. Gong, Z. Li, S. Tao, Q. Jiang, D. Jiang, *Angew. Chem. Int. Ed.* **2020**, *59*, 5050–5091; *Angew. Chem.* **2020**, *132*, 5086–5129; b) L.-H. Li, X.-L. Feng, X.-H. Cui, Y.-X. Ma, S.-Y. Ding, W. Wang, *J. Am. Chem. Soc.* **2017**, *139*, 6042–6045.

[4] a) Q. Guan, L.-L. Zhou, Y.-B. Dong, *Chem. Soc. Rev.* **2022**, *51*, 6307–6416; b) X. Kan, J.-C. Wang, Z. Chen, J.-Q. Du, J.-L. Kan, W.-Y. Li, Y.-B. Dong, *J. Am. Chem. Soc.* **2022**, *144*, 6681–6686; c) C.-J. Wu, X.-Y. Li, T.-R. Li, M.-Z. Shao, L.-J. Niu, X.-F. Lu, J.-L. Kan, Y. Geng, Y.-B. Dong, *J. Am. Chem. Soc.* **2022**, *144*, 18750–18755; d) X. Wang, M.-J. Dong, C.-D. Wu, *Nanoscale* **2020**, *12*, 16136–16142.

[5] a) E. Jin, M. Asada, Q. Xu, S. Dalapati, M. A. Addicoat, M. A. Brady, H. Xu, T. Nakamura, T. Heine, Q. Chen, D. Jiang, *Science* **2017**, *357*, 673–676; b) X. Li, *Mater. Chem. Front.* **2021**, *5*, 2931–2949.

[6] H. Wang, H. Wang, Z. Wang, L. Tang, G. Zeng, P. Xu, M. Chen, T. Xiong, C. Zhou, X. Li, D. Huang, Y. Zhu, Z. Wang, J. Tang, *Chem. Soc. Rev.* **2020**, *49*, 4135–4165.

[7] W. Zhong, R. Sa, L. Li, Y. He, L. Li, J. Bi, Z. Zhuang, Y. Yu, Z. Zou, *J. Am. Chem. Soc.* **2019**, *141*, 7615–7621.

[8] a) M. Traxler, S. Gisbertz, P. Pachfule, J. Schmidt, J. Roeser, S. Reischauer, J. Rabeah, B. Pieber, A. Thomas, *Angew. Chem. Int. Ed.* **2022**, *61*, e202117738; *Angew. Chem.* **2022**, *134*, e202117738; b) W. Dong, Y. Yang, Y. Xiang, S. Wang, P. Wang, J. Hu, L. Rao, H. Chen, *Green Chem.* **2021**, *23*, 5797–5805; c) H. Chen, W. Liu, A. Laemont, C. Krishnaraj, X. Feng, F. Rohman, M. Meledina, Q. Zhang, R. Van Deun, K. Leus, P. Van Der Voort, *Angew. Chem. Int. Ed.* **2021**, *60*, 10820–10827; *Angew. Chem.* **2021**, *133*, 10915–10922; d) H. Chen, H. S. Jena, X. Feng, K. Leus, P. Van Der Voort, *Angew. Chem. Int. Ed.* **2022**, *61*, e202204938; *Angew. Chem.* **2022**, *134*, e202204938.

[9] A. Y. Chan, I. B. Perry, N. B. Bissonnette, B. F. Buksh, G. A. Edwards, L. I. Frye, O. L. Garry, M. N. Lavagnino, B. X. Li, Y. Liang, E. Mao, A. Millet, J. V. Oakley, N. L. Reed, H. A. Sakai, C. P. Seath, D. W. C. MacMillan, *Chem. Rev.* **2022**, *122*, 1485–1542.

[10] a) Z. Zuo, D. T. Ahneman, L. Chu, J. A. Terrett, A. G. Doyle, D. W. C. MacMillan, *Science* **2014**, *345*, 437–440; b) J. Twilton, C. Le, P. Zhang, M. H. Shaw, R. W. Evans, D. W. C. MacMillan, *Nat. Chem. Rev.* **2017**, *1*, 0052; c) E. R. Welin, C. Le, D. M. Arias-Rotondo, J. K. McCusker, D. W. C. MacMillan, *Science* **2017**, *355*, 380–385; d) M. Kudisch, C.-H. Lim, P. Thordarson, G. M. Miyake, *J. Am. Chem. Soc.* **2019**, *141*, 19479–19486.

[11] S. I. Ting, S. Garakyaraghi, C. M. Taliaferro, B. J. Shields, G. D. Scholes, F. N. Castellano, A. G. Doyle, *J. Am. Chem. Soc.* **2020**, *142*, 5800–5810.

[12] J. Li, C.-Y. Huang, C.-J. Li, *Chem* **2022**, *8*, 2419–2431.

[13] R. Bu, L. Zhang, X.-Y. Liu, S.-L. Yang, G. Li, E.-Q. Gao, *ACS Appl. Mater. Interfaces* **2021**, *13*, 26431–26440.

[14] L. Zhang, L. Jiao, *J. Am. Chem. Soc.* **2017**, *139*, 607–610.

[15] M. Jiang, H. Yang, H. Fu, *Org. Lett.* **2016**, *18*, 5248–5251.

[16] D.-L. Zhu, R. Xu, Q. Wu, H.-Y. Li, J.-P. Lang, H.-X. Li, *J. Org. Chem.* **2020**, *85*, 9201–9212.

Manuscript received: December 21, 2022
Accepted manuscript online: January 18, 2023
Version of record online: ■■, ■■

Communications

Covalent Organic Frameworks

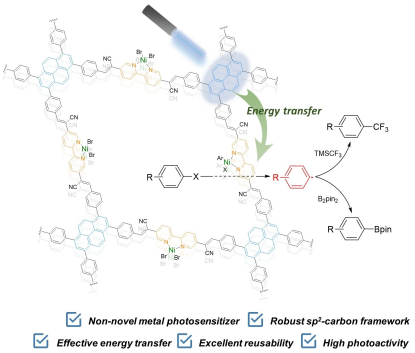

This work describes excited-state nickel-catalyzed borylation and trifluoromethylation reactions in a covalent organic framework (COF). Rapid energy transfer in the sp^2-carbon conjugated COF facilitates the generation of aryl radicals from nickel-aryl complexes, leading to two orders of magnitude higher catalytic efficiency than the homogeneous counterpart in aryl borylation and trifluoromethylation reactions.